metals

MDPI

Article

Characterization of In-Situ Cu–TiH2–C and Cu–Ti–C Nanocomposites Produced by Mechanical Milling and Spark Plasma Sintering

Nguyen Thi Hoang Oanh [1,*], Nguyen Hoang Viet [1], Ji-Soon Kim [2] and Alberto Moreira Jorge Junior [3,4,5,6,7]

1 School of Materials Science and Engineering, Hanoi University of Science and Technology, No. 1 Dai Co Viet, Hanoi 100000, Vietnam; viet.nguyenhoang@hust.edu.vn
2 School of Materials Science and Engineering, University of Ulsan, San-29, Mugeo-2 Dong, Nam-Gu, Ulsan 680-749, Korea; jskim@ulsan.ac.kr
3 Department of Materials Science and Engineering, Federal University of São Carlos, Via Washington Luiz, km 235, São Carlos, SP 13565-905, Brazil; Jorge.Moreira@simap.grenoble-inp.fr
4 University of Grenoble Alpes, Science et Ingénierie des Matériaux et Procédés (SIMAP), F-38000 Grenoble, France
5 Centre National de la Recherche Scientifique (CNRS), Science et Ingénierie des Matériaux et Procédés (SIMAP), F-38000 Grenoble, France
6 University of Grenoble Alpes, Laboratoire d'Electrochimie et de Physico-chimie des Matériaux et des Interfaces (LEPMI), F-38000 Grenoble, France
7 Centre National de la Recherche Scientifique (CNRS), Laboratoire d'Electrochimie et de Physico-chimie des Matériaux et des Interfaces (LEPMI), F-38000 Grenoble, France
* Correspondence: oanh.nguyenthihoang@hust.edu.vn; Tel.: +84-4-3868-0409

Academic Editor: Manoj Gupta
Received: 5 February 2017; Accepted: 27 March 2017; Published: 29 March 2017

Abstract: This study focuses on the fabrication and microstructural investigation of Cu–TiH2–C and Cu–Ti–C nanocomposites with different volume fractions (10% and 20%) of TiC. Two mixtures of powders were ball milled for 10 h, consequently consolidated by spark plasma sintering (SPS) at 900 and 1000 °C producing bulk materials with relative densities of 95–97%. The evolution process of TiC formation during sintering process was studied by using X-ray diffraction (XRD), scanning electron microscopy (SEM), and high resolution transmission electron microscopy (HRTEM). XRD patterns of composites present only Cu and TiC phases, no residual Ti phase can be detected. TEM images of composites with (10 vol % TiC) sintered at 900 °C show TiC nanoparticles about 10–30 nm precipitated in copper matrix, most of Ti and C dissolved in the composite matrix. At the higher sintering temperature of 1000 °C, more TiC precipitates from Cu–TiH2–C than those of Cu–Ti–C composite, particle size ranges from 10 to 20 nm. The hardness of both nanocomposites also increased with increasing sintering temperature. The highest hardness values of Cu–TiH2–C and Cu–Ti–C nanocomposites sintered at 1000 °C are 314 and 306 HV, respectively.

Keywords: spark plasma sintering; Cu–TiC; in-situ composites; mechanical milling

1. Introduction

Metal matrix composites (MMCs) are advanced materials which combine ductility and toughness of metal and high strength and modulus of ceramic particles. The unique properties of MMCs are high specific strength, specific modulus, and good wear resistance compare to unreinforced metal [1]. In many type of MMCs, copper matrix composites (CMCs) have received a lot of interest because of super toughness and wear resistance which are used for structural application in wear industry [2].

Generally, there are two routes to produce particulate-reinforced CMCs, which are ex-situ and in-situ. In the ex-situ method, ceramic particles such as TiB2, TiC, and oxide are introduced into the metal matrix via powder metallurgy or conventional casting methods [3,4]. However, the CMCs fabricated by these methods revealed a drawback because of poor interfacial bonding between reinforcement particles and copper matrix [5]. In order to improve the wettability of the Cu matrix and reinforcement phase, nano-ceramic particles were used [6]. Nevertheless, ceramic nanoparticles have tendency to segregate into clusters in milling process leading decrease strength of composite. The distribution of reinforced particles are non-uniform in the copper matrix, the mechanical and electrical features of the composite will be affected negatively [7]. On the contrary, ceramic particles synthesized by the in-situ method were dispersed more homogeneously in the copper matrix. The interfaces between reinforcement particles and matrix are clean, and very fine reinforcement particles are formed. Among CMCs, Cu–TiC system is attracted more attention due to their potential applications as electrical sliding contacts, resistance welding electrodes [8]. In the in-situ method, TiC nanoparticles were produced by the reaction between Ti and C during sintering process. In order to prevent grain growth of reinforcement and copper particles occur at high sintering temperature a fast sintering process need to be carried out. Spark plasma sintering (SPS) has some advantages such as rapid sintering, uniform sintering, low running cost, easy operation proves a suitable sintering technique for consolidation nano-structure, nanocomposite, and amorphous materials. In SPS, very high temperature over melting temperature may be attained in the contact area of powder particles which enhances interparticle bonding without considerable grain growth occurring [9–13].

The replacement of Ti powder in Cu–Ti–C composite by another powder such as TiH2 is considerable because of high price of Ti powder. In addition to, dehydrogenation of TiH2 occurs during sintering process is always accompanied by formation of high concentration of lattice defects and the highly activated Ti atoms. Released hydrogen from TiH2 will react with oxygen on the surface of TiH2 powders in the form of H2O which affect positively on the electrical conductivity of the composite [14].

The objectives of the present work are to explore the possibility of synthesizing Cu–TiC in-situ composites made from Cu–TiH2–C and Cu–Ti–C powder mixtures by mechanical milling and SPS. The effect of reinforcement content and sintering temperature on microstructure and hardness properties of composites was investigated.

2. Experimental Procedure

The copper (with average particle size of 75 μm), titanium (average particle size of 45 μm), TiH_2 (average particle size of 40 μm) and graphite (average particle size of 5 μm) powder (≥99% purity, from HIGH PURITY CHEMICALS Co., Ltd., Chiyoda, Japan) were used as starting materials. The powder mixtures of two composites Cu–TiH2–C and Cu–Ti–C with mixing ratio of 10 and 20 vol % TiC were mechanically milled in a high-energy planetary ball mill (P100-Korea). Milling was operated for 10 h at the rotational speed of 500 rpm and 0.5 wt % stearic acid was used as the milling process control agent. Balls and vials are made of stainless steel, the diameter of the balls was 5 mm and the powder-to-ball ratio was 1:10. The vial was evacuated and subsequently filled with argon up to 0.3 MPa.

A 1.5 g amount of as-milled powder was loaded into a cylindrical graphite die with 10 mm-inner and was subjected to a pulsed current using a spark plasma sintering equipment, (SPS-515 apparatus Sumitomo Coal Mining, Tokyo, Japan). The chamber was pumped to low vacuum (<5 Pa). The composite powders were spark plasma sintered at 900 and 1000 °C under a pressure of 50 MPa for 5 min with a heating rate of 50 °C/min.

X-ray diffraction patterns of the composites were recorded by a SIEMENS D5000 diffractometer (Siemens Industry Inc., Karlsruhe, Germany) using Cu K_α radiation (λ = 1.5418 Å). Microstructural analysis of powders and composite samples was carried out by using Scanning Electron Microscopy (SEM/EDX-JEOL JSM-7600F, JEOL Ltd., Tokyo, Japan) and Transmission Electron Microscopy (TEM-JEOL JEM-2100, JEOL Ltd., Tokyo, Japan). Relative densities of bulk composites were determined

by Archimedes method. The indexation of such selected area electron diffraction (SAED) patterns was performed using JEMS software [15].

Microhardness measurements were performed using a Vickers hardness instrument (Mitutoyo MVK-H1 Hardness Testing Machine, Mitutoyo, Japan) under a load of 100 g.

To analyze the surface of fracture, samples were simply fractured by gripping the halves of the composite with pliers and bending them apart.

3. Results and Discussion

3.1. Characterization of the Powders

Figure 1a,b shows SEM images of starting powders, respectively for TiH_2 and copper powders. TiH_2 particles have an irregular shape while Cu powder particles have a dendritic shape. Figure 1c–f show SEM images of composite powders formed after 10 h of milling of Cu–TiH2–C and Cu–Ti–C mixtures, with different amounts of reinforcement particle content. As one can observe, the increase of the reinforcement particle content the particle size of milled powders decreases for both composites. Cu–Ti–C composite presented finer particles than those for the Cu–TiH2–C composite, with the same reinforcement particle content. As can be seen from SEM images shown in Figure 1g,h. Some large particles were formed due to agglomeration of small particles reaching a size of 10–30 µm. EDS analyses (Figure 2) were performed on particles such as in Figure 1g,h which presents spectra relative to such analyses, of which it is worth noting that there was no contamination of Fe either from the milling tools (Table 1). However, such contamination was already observed even in the ex-situ method as reported in [16].

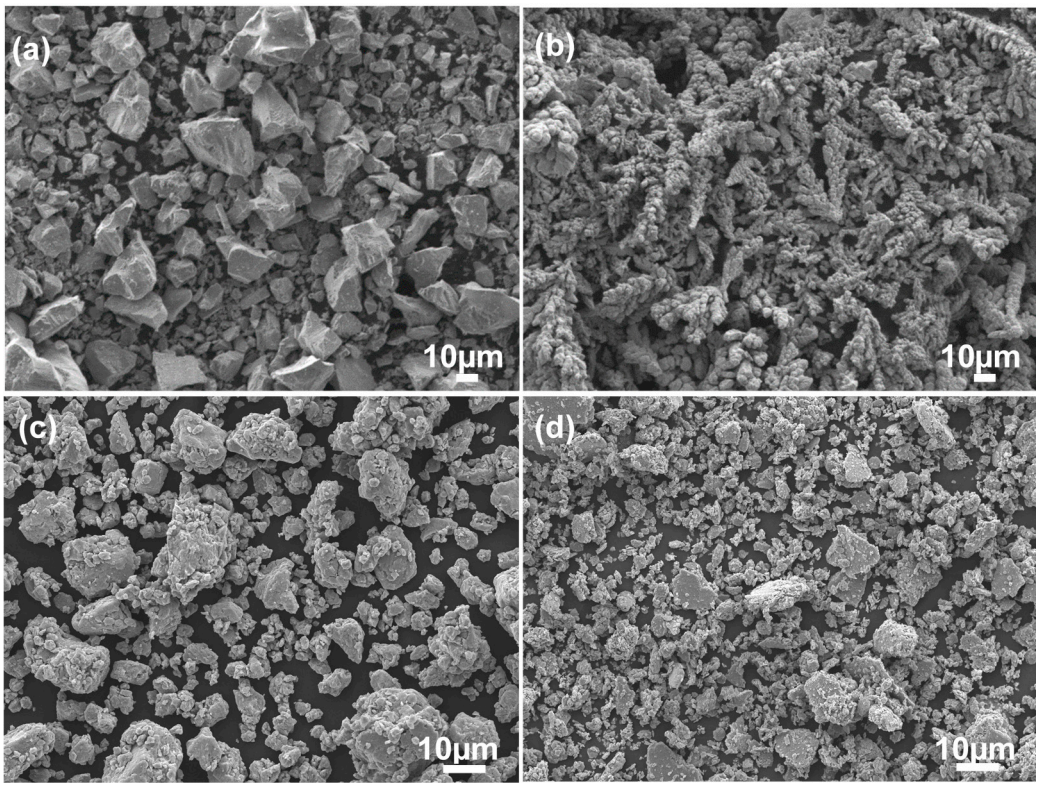

Figure 1. *Cont.*

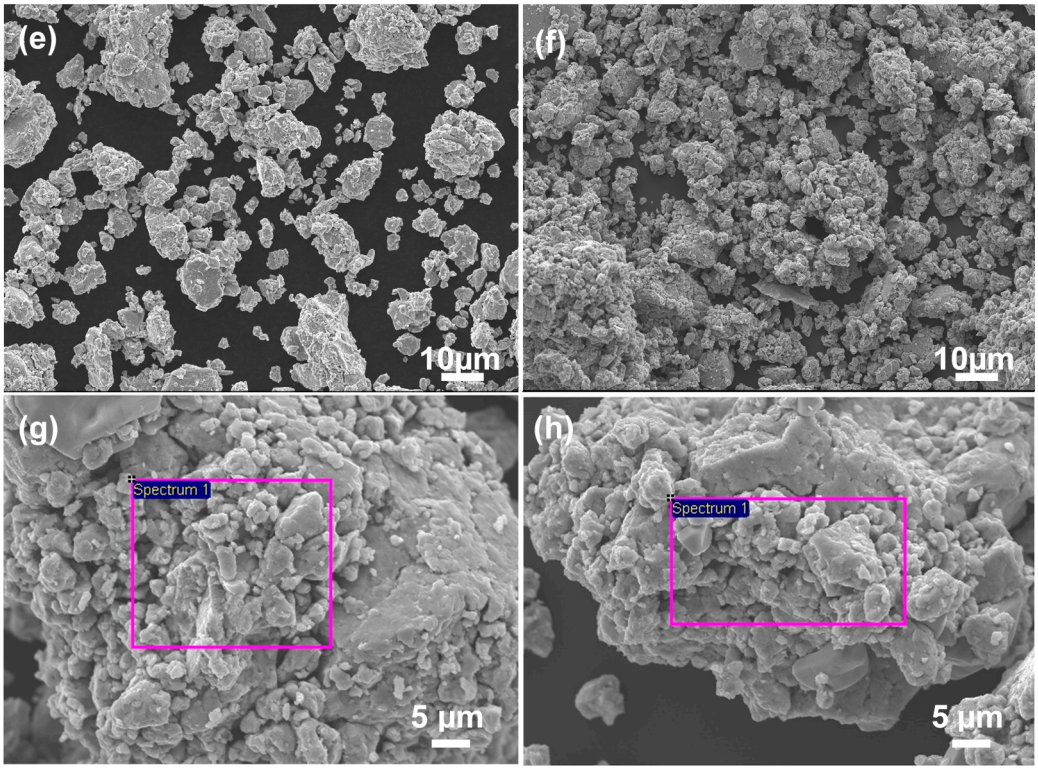

Figure 1. SEM of starting powders in (**a**) TiH_2 and (**b**) copper powders. SEM images of composite powders milled for 10 h, with 10 vol % TiC in (**c**) Cu–TiH2–C and (**d**) Cu–Ti–C; and with 20 vol % TiC in (**e**) Cu–TiH2–C and (**f**) Cu–Ti–C. Higher-magnification SEM images; the rectangles mark areas; from which EDS spectra were taken (**g**) Cu–TiH2–C and (**h**) Cu–Ti–C.

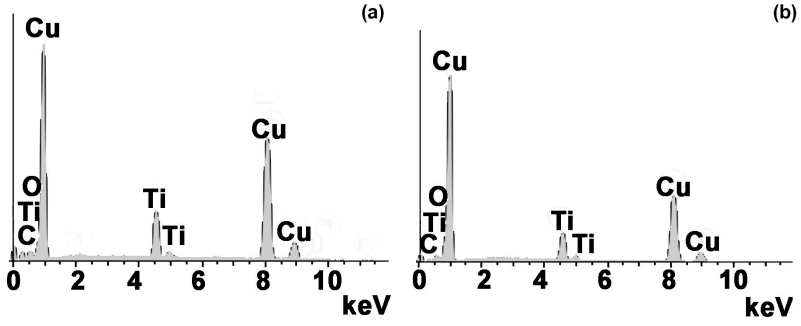

Figure 2. Typical EDS analyses acquired from particles presented in Figure 1e (Cu–Ti–C) in (**a**) and Figure 1f (Cu–TiH2–C) in (**b**), both with 20 vol % TiC.

Table 1. EDS analysis of the ball milled powders with 20 vol % of TiC reinforcement particles.

Composite	Concentration, wt %			
	Cu	Ti	C	O
Cu–TiH2–C	73.78	8.75	13.42	4.05
Cu–Ti–C	70.73	7.89	16.49	4.89

3.2. Characterization of Compacts after SPS

X-ray diffraction patterns of as-sintered nanocomposites are illustrated in Figure 3. After SPS at 900 °C (Figure 3a), XRD patterns presents only diffraction peaks related to pure copper. There

is a shift peak of copper in sintered composite compare to starting Cu powder. This fact clearly evidences that most of the Ti and C have dissolved in the copper matrix and also that the sintering temperature was not high enough to precipitate the TiC phase. Conversely, by increasing the sintering temperature to 1000 °C, Ti reacts with C, and TiC precipitates, as it is clearly noticeable in the XRD patterns of Figure 3b for mixtures with 20 vol % TiC. However, there is reason to believe that the same has occurred for mixtures with 10 vol % of TiC because this is a thermodynamical condition. TiC weight percentages in bulk composites sintered at 1000 °C produced from starting powders was calculated by Rietveld refinement method as shown in Table 2. The weight percentages of in-situ TiC nanoparticles with 10 vol % reinforcement particles for Cu–TiH2–C and Cu-Ti–C composites are 1.43 and 2.86%, respectively. Furthermore, as it will be under mentioned, TEM analyses confirm the presence of TiC nanoparticles in mixtures with 10 vol % of TiC. At higher reinforcement particles of 20 vol %, the amount of TiC precipitated from Cu–TiH2–C and Cu-Ti–C composites also increases to 6.9 and 6.45 wt %, respectively. Additionally, it is important to observe that there was no precipitation of intermetallic phases during sintering process at any of the sintering temperatures. If one considers the Cu–Ti–C system, normally Cu, Ti, and C may interact to form several products through chemical reactions [17]. However, the Gibbs free energy of TiC formation at the temperature of 1273 K is about 84.4 kJ/mol, which is much lower than those to form other intermetallic phases of Ti and Cu, implying that the precipitation of TiC is thermodynamically preferred relative to other possible reactions.

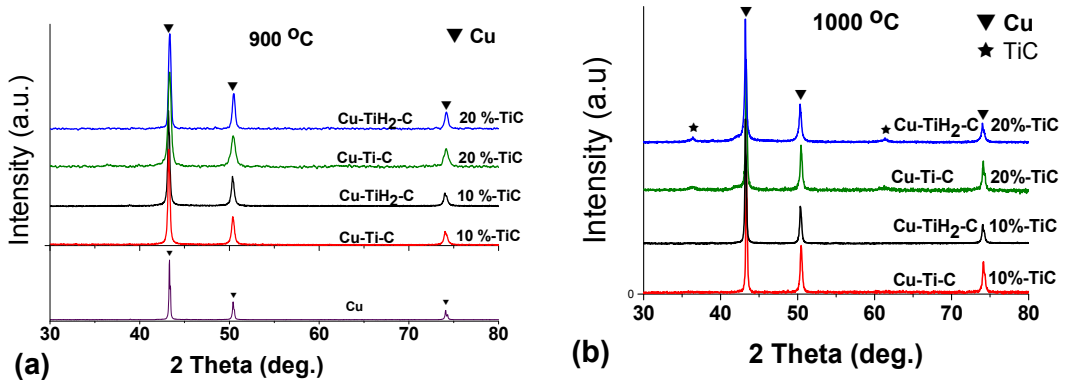

Figure 3. XRD patterns of nanocomposites (**a**) Spark Plasma Sintered at 900 °C; (**b**) Spark Plasma Sintered at 1000 °C.

Table 2. Fraction of phases of Cu–TiH2–C and Cu–Ti–C composites sintered at 1000 °C calculated by Rietveld refinement.

Phase	Fraction of Phases (%)			
	Cu–TiH2–C		Cu–Ti–C	
	10 vol % TiC	20 vol % TiC	10 vol % TiC	20 vol % TiC
TiC	2.86	6.9	1.43	6.45
Cu	97.14	97.14	98.57	93.55

Figure 4a–d present backscattered electron (BSE) SEM images of Cu–TiH2–C and Cu–Ti–C nanocomposites sintered at 1000 °C, showing details of the surface of samples. From these images, one can observe the presence of three gray tones, where black regions indicate the presence of some closed porosity on the surface, dark-gray regions correspond to the solid solution Cu(Ti, C), and, finally, white regions correspond to Cu-richer regions. It is interesting to note that the porosity is minimal for Cu–TiH2–C nanocomposites for any amount of TiC. The porosity increases for Cu–Ti–C nanocomposites but reduces by increasing the amount of TiC. However, apparently, Cu-richer regions are thinner and better distributed for Cu–Ti–C nanocomposites than for Cu–TiH2–C ones, diminishing

with the amount of TiC. Conversely, the thicker and worse distributed Cu-richer regions in Cu–TiH2–C nanocomposites augment with the amount of TiC.

Relative density measurements, presented in Table 3, confirm the above results regarding porosity. The relative density of the Cu–TiH2–C and Cu–Ti–C nanocomposites increases as the sintering temperature increases from 900 to 1000 °C. Therefore, one could infer that this fact may be due to the enhanced viscosity of Cu/Cu(Ti, C) matrix at the higher sintering temperature, which results in an efficient filling of pores due to high diffusion rates. In composites produced in-situ, the interfacial area is higher compared to ex-situ composites, detrimental effects of interfacial phenomena (decohesion, void formation) are more likely to prevail at high sintering temperatures compared to low sintering temperatures. Islak et al. [7] reported that in hot-pressed Cu–Ti–C nanocomposites, with 10 vol % TiC, the highest relative density obtained was about 86.4%, while in our samples, with the same TiC content, it is, on average, around 96.8 either for Cu–TiH2–C or Cu–Ti–C nanocomposites sintered at 1000 °C. The presence of porosity on the surface of nanocomposites is a natural result of the consolidation process. The relative density of Cu–TiH2–C has higher than that of Cu–Ti–C composite that why the amount of porosity can be seen in Figure 4b,d is more than in Figure 4a,c, respectively. The maximum relative density values were measured for Cu–TiH2–C and Cu–Ti–C nanocomposites at the sintering temperature of 1000 °C with 10 vol % TiC, which were 97% and 96.6%, respectively.

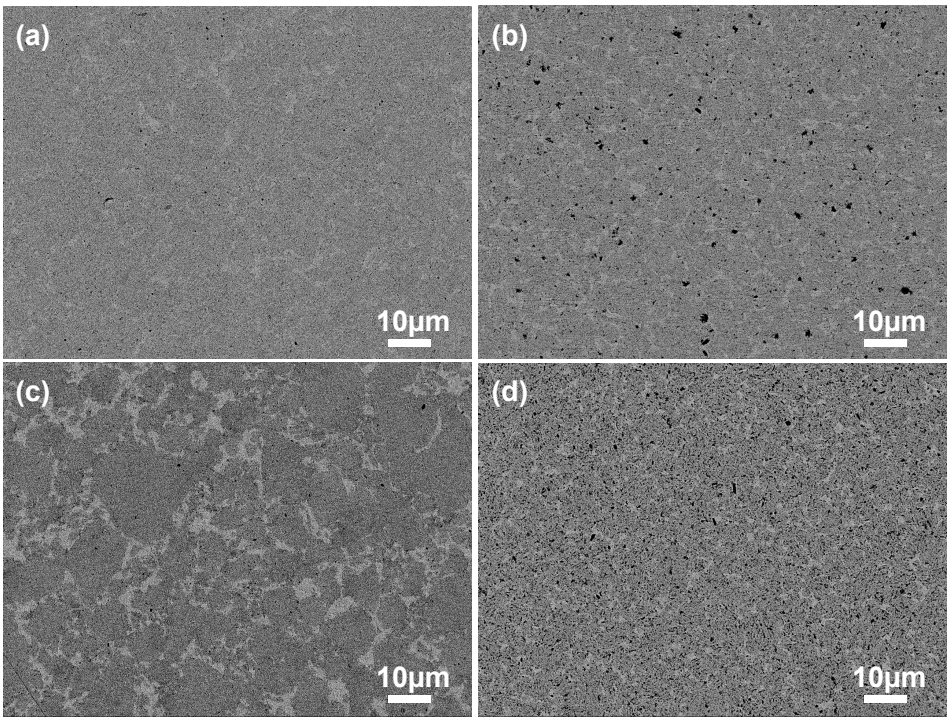

Figure 4. SEM images of Cu–TiH2–C and Cu–Ti–C nanocomposites Spark Plasma Sintered at 1000 °C: (**a**) 10 vol % TiC, Cu–TiH2–C nanocomposite; (**b**) 10 vol % TiC, Cu–Ti–C nanocomposite; (**c**) 20 vol % TiC, Cu–TiH2–C nanocomposite; (**d**) 20 vol % TiC, Cu–Ti–C nanocomposite.

Table 3. Relative density of Spark plasma sintered Cu–TiH2–C and Cu–Ti–C nanocomposites.

Sintering Temperature (°C)	Relative Density (%)			
	Cu–TiH2–C		Cu–Ti–C	
	10 vol % TiC	20 vol % TiC	10 vol % TiC	20 vol % TiC
900	95.8	95.3	95.4	95.2
1000	97.0	96.4	96.6	96.2

Figure 5 displays TEM images of Cu–TiH2–C nanocomposites with 10 vol % TiC and sintered at 900 °C. As one can observe, Ti still continues in the matrix, having a particle size of about 50 nm. Figure 5a shows some TiC nanograins of about 10–20 nm precipitated near Ti particles. As stated before, the reaction between Ti and C is not complete because the sintering temperature is not high enough to enhance the diffusion of C into Ti. Thus most of Ti and C remains in the composite matrix. Figure 5c–e presents examples of selected area electron diffraction (SAED) patterns of Cu–TiH2–C nanocomposite showing diffraction patterns for Cu, Ti, and TiC particles. There is a small misfit in the indexation of Cu due to the presence of Ti and C in solution into the copper. In addition, there are extra spots in SAEDs because of particle sizes. As the particles are smaller than the smallest aperture, the diffraction will be taken from the particle and regions around. At the sintering temperature of 1000 °C, TiC particles precipitate copiously on the nanocomposite matrix with particles size ranging between 10 and 30 nm as shown in Figure 6a,b. No other phase containing Ti could be detected under the TEM resolution.

Figure 6c,d present TEM images of Cu–Ti–C nanocomposites, with 10 vol % TiC, and sintered at 900 °C, showing few TiC nanoparticles with sizes ranging between 10 to 30 nm. As it occurred for Cu–TiH2–C nanocomposites, at the low sintering temperature of 900 °C, only a small fraction of Ti will react with C, and most of Ti and C continue dissolving in the composite matrix. At the sintering temperature of 1000 °C (Figure 6e,f), more TiC precipitates, whose particle size ranges from 10 to 20 nm. Nevertheless, Ti is still observed in the HRTEM image presented in Figure 6f.

The presence of TiC, even in mixtures with 10 vol % of TiC at high sintering temperature during XRD analyses (Figure 3), is confirmed by the observation that TiC precipitates in the TEM analysis.

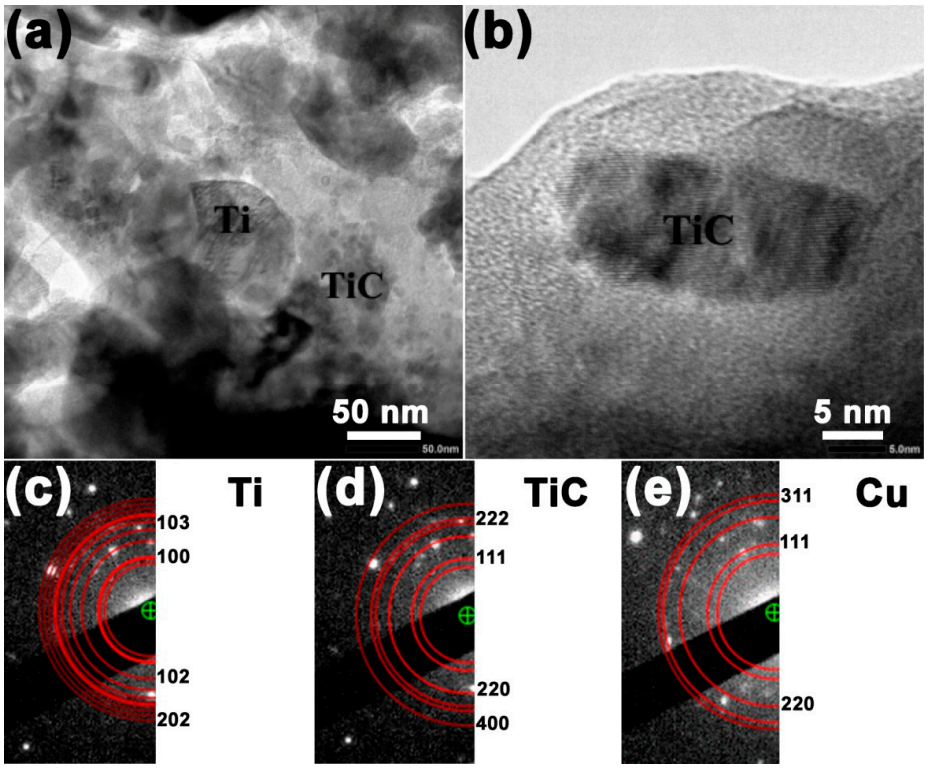

Figure 5. TEM images and SAED of Cu–TiH2–C nanocomposites of 10 vol % TiC sintered at 900 °C: (**a**) bright-field image; (**b**) HR-TEM image of TiC crystal on copper matrix; (**c**) SAED of Ti; (**d**) SAED of TiC; and (**e**) SAED of copper.

As it can be observed in Figures 5 and 6, the amount of TiC precipitated in the Cu–TiH2–C nanocomposite is higher than that for Cu–Ti–C after sintering at 1000 °C. Yang et al. [14] also prepared bulk TiC from TiH_2–C and Ti–C by self-propagation high-temperature synthesis method. By XRD and

DSC results, they found that for TiH_2–C, Ti and C reacted to produce TiC in the temperature range of 1130 to 1300 °C, very small amount of Ti remained after SHS process. For Ti–C, only an endothermic peak appears at 880 °C because of the α-Ti transformation to β-Ti and a lot of Ti and C remain. Little TiC is detected, but the amount is much smaller than TiH_2–C.

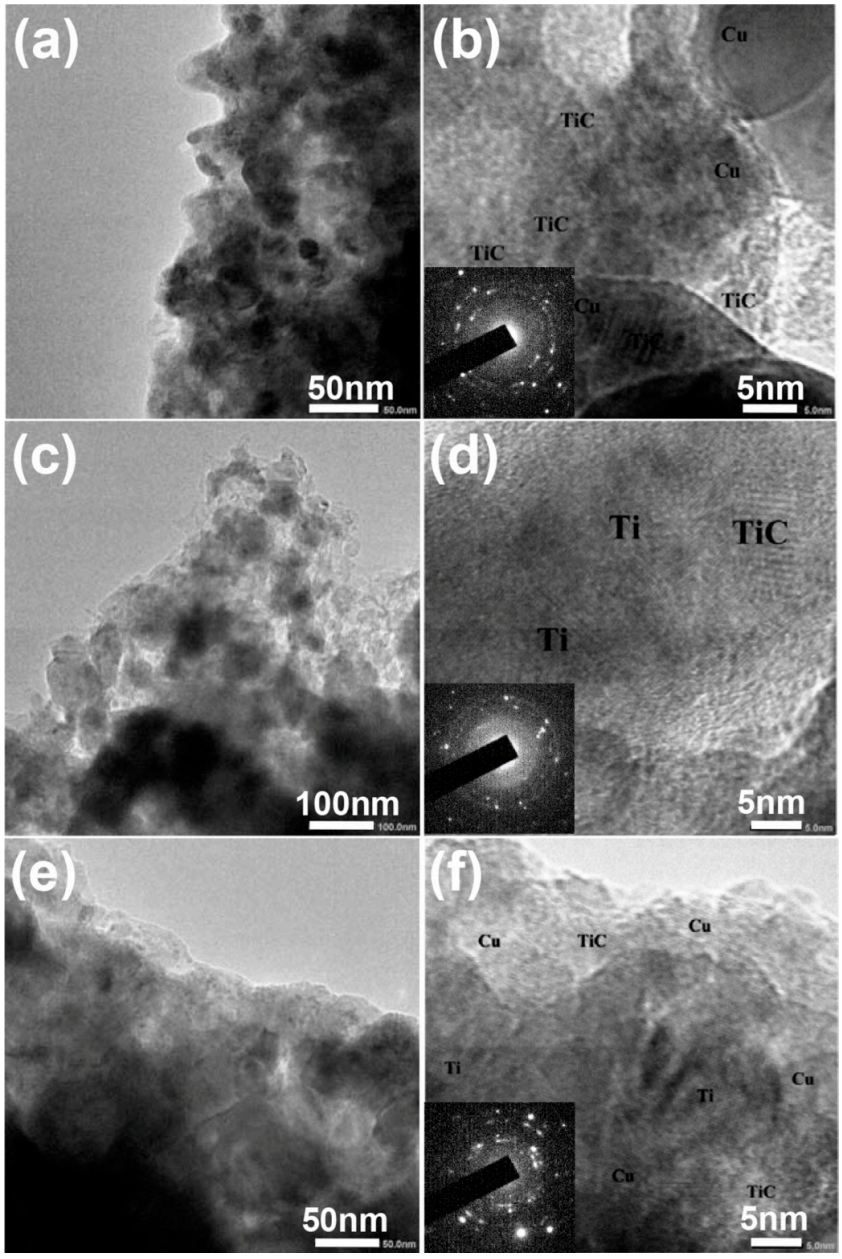

Figure 6. TEM images of: Cu–TiH2–C nanocomposite—10 vol %TiC and sintered at 1000 °C, bright-field image in (**a**) and HR-TEM image in (**b**); Cu–Ti–C nanocomposite—10 vol %TiC and sintered at 900 °C, bright-field image in (**c**) and HRTEM image in (**d**); Cu–Ti–C nanocomposite—10 vol %TiC and sintered at 1000 °C, bright-field image in (**e**) and HRTEM image in (**f**), SAEDs refer to TiC particles.

3.3. Hardness Results of Compacts

The hardness of a composite is an important parameter that determines their wear resistance for sliding contact applications. In this sense, hard TiC particles play an important role when reinforcing the soft Cu matrix. These particles lead to a higher hardness of the composite. Table 4 summarizes hardness values for all conditions studied in this work. From this table, it is possible to observe that,

at the sintering temperature of 900 °C, hardness values of Cu–Ti–C nanocomposites are lower than those for Cu–TiH2–C nanocomposites, for any addition of TiC. The formation of Cu(Ti, C) solid solution enhances the hardness of the composites. As the sintering temperature increases, there is a significant increase in the hardness values because more TiC particles precipitate after the reaction between Ti and C. The highest hardness value of an ex-situ Cu–Ti–C composite with 10 vol % of TiC was found to be about 86.4 HV [7], much lower than those found for the in-situ produced nanocomposites of this work, which were 295 and 290 HV respectively for Cu–TiH2–C and Cu–Ti–C nanocomposites with the same TiC content and sintered at 900 °C. By increasing the volume of TiC, the hardness of nanocomposites also increases to 314 and 306 HV correspondingly for Cu–TiH2–C and Cu–Ti–C nanocomposites when sintered at 1000 °C.

Table 4. Hardness values of nanocomposites sintered at 900 and 1000 °C.

Sintering Temperature (°C)	Hardness Value, HV			
	Cu–TiH2–C		Cu–Ti–C	
	10 vol % TiC	20 vol % TiC	10 vol % TiC	20 vol % TiC
900	250	245	242	244
1000	295	314	290	306

3.4. Fracture Analysis

Figure 7 presents fracture morphologies of nanocomposites with 10 vol % TiC. The presence of dimples on the fracture surface suggests a ductile fracture mode in both nanocomposites Cu–TiH2–C and Cu–Ti–C. Fracture surface of the composites exhibits nano-void and micro-void coalescence in the matrix. Gray ultrafine particles are embedded in the copper matrix, which are fracture paths along grain boundaries of the matrix.

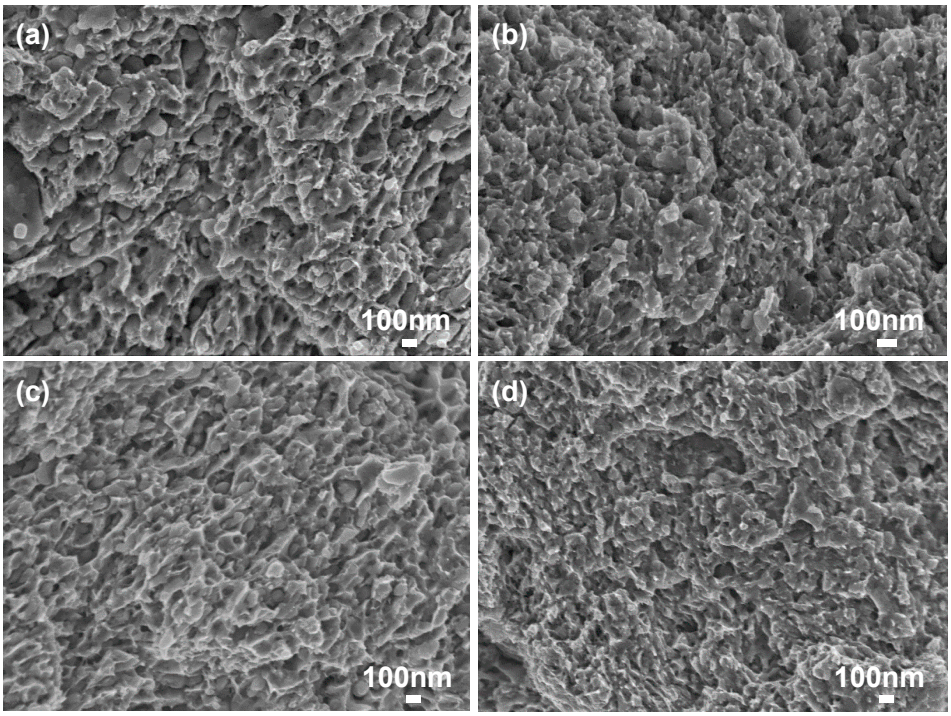

Figure 7. Fracture surfaces of 10 vol. %TiC (**a**) Cu–TiH2–C nanocomposite sintered at 900 °C; (**b**) Cu–Ti–C nanocomposite sintered at 900 °C; (**c**) Cu–TiH2–C nanocomposite sintered at 1000 °C; and (**d**) Cu–Ti–C nanocomposite sintered at 1000 °C.

At the highest sintering temperature of 1000 °C, one can observe a better contact between reinforcement particles and matrix, as presented in Figure 7c,d. The dimple size decreases with an increase in TiC content from 10 to 20 vol % as seen in Figure 8. The presence of more reinforcement particle content in the copper matrix prevents dimple growth. The fracture behavior of these nanocomposites also depicts a mixed mode, with the brittle mode of fracture being the predominant one. The fracture surface of both composites indicate nearly flat surface, minimal plastic deformation preceding the fracture occurs. The microscopic characteristics include faceted surface and transgranular fracture of Cu grains in the composites.

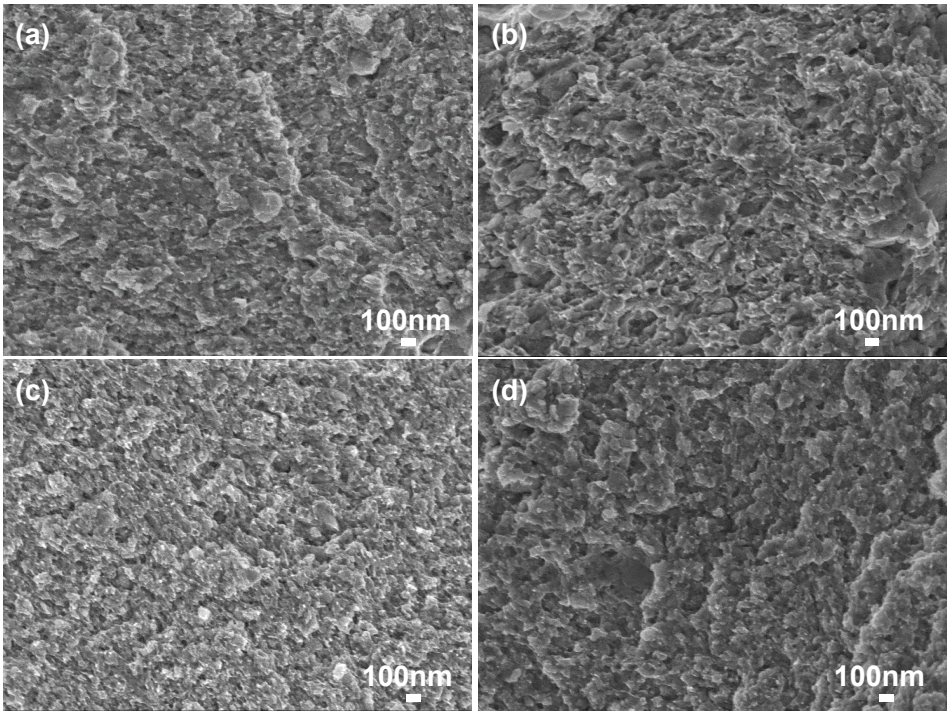

Figure 8. Fracture surfaces of 20 vol % TiC (**a**) Cu–TiH2–C nanocomposite sintered at 900 °C; (**b**) Cu–Ti–C nanocomposite sintered at 900 °C; (**c**) Cu–TiH2–C nanocomposite sintered at 1000 °C; and (**d**) Cu–Ti–C nanocomposite sintered at 1000 °C.

In order to investigate the distribution of reinforcing particulates in copper matrix, EDS analyses for the composite sintered at 1000 °C with 10 vol % TiC, is presented in Figure 9. The size of the "waves" on the Ti and C concentration profiles along the x-axis (distance) corresponds well to the size of the TiC nanoparticles introduced into the copper matrix through ball milling. The distribution of the Ti and C through copper matrix in Cu–TiH2–C is better than of Cu–Ti–C. The content of oxygen in Cu–TiH2–C is lower than Cu–Ti–C composite which means that the effect of hydrogen release from TiH_2 reacts with the oxygen lead to reduce the oxygen content in the composite after sintering. No contamination such as Fe from the balls and jar can be detected for both composites.

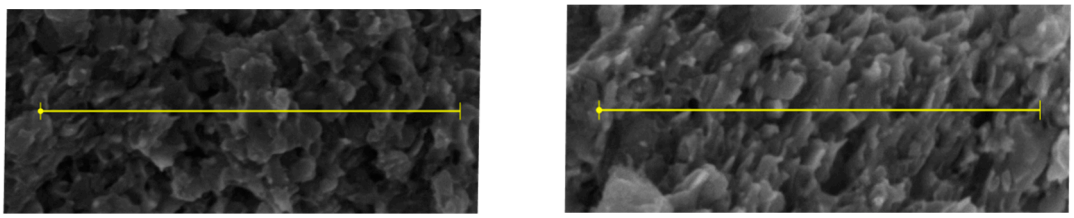

Figure 9. *Cont.*

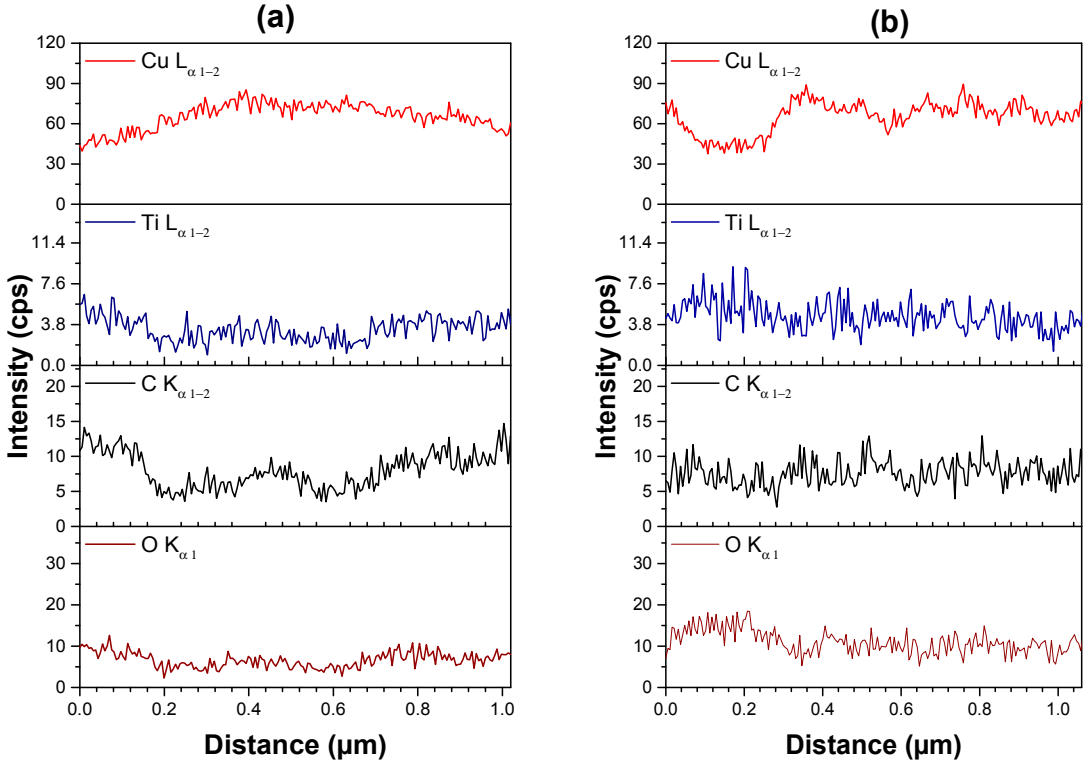

Figure 9. SEM images and EDS profiles for (**a**) Cu–TiH2–C and (**b**) Cu–Ti–C composites sintered at 1000 °C with 10 vol % reinforcement particles.

4. Conclusions

In-situ copper matrix composites strengthened with (10 and 20 vol %) TiC were prepared by SPS of ball milled mixtures of Cu–TiH2–C and Cu–Ti–C powders. The relative densities of composites sintered at 900 and 1000 °C are in the range of 95%–97%. The XRD of composites sintered at 900 °C showed only Cu(Ti, C) solid solution, no trace of TiC or oxide phases. Increasing sintering temperature to 1000 °C, diffraction peaks of TiC and pure Cu phases can be seen from XRD patterns for composites reinforced with 20 vol % TiC, while for composite with 10 vol % TiC reinforcement no diffraction peaks of TiC phase can be detected. The results of TEM analysis for these composites confirmed the presence of nanoparticle TiC about 10 to 20 nm disperse on Cu matrix near residual Ti particles whereas, under XRD resolution, it cannot detected. A larger amount of TiC nanoparticles precipitated in the Cu–TiH2–C composite is observed than for that of Cu–Ti–C from TEM images. These TiC nanoparticles enhance the hardness of composites prepared from the former. With the increasing the reinforcement particles content from 10 to 20 vol % the hardness values of composites increased while relative density slightly decreased. The hardness of composites also increased with increasing sintering temperature with any reinforcement particles addition. The highest hardness values of Cu–TiH2–C and Cu–Ti–C composites sintered at 1000 °C are 314 and 306 HV, respectively.

Acknowledgments: This research was funded by the Vietnam National Foundation for Science and Technology Development (NAFOSTED), grant number 103.02-2011.49.

Author Contributions: Nguyen Thi Hoang Oanh and Nguyen Hoang Viet designed the research, conducted the experiments, and wrote the paper. Ji-Soon Kim supervised the project and Alberto Moreira Jorge Junior revised the manuscript. All authors reviewed the manuscript.

Conflicts of Interest: The authors declare no conflict of interest.

References

1. Shirvanimoghaddam, K.; Hamim, S.U.; Karbalaei Akbari, M.; Fakhrhoseini, S.M.; Khayyam, H.; Pakseresht, A.H.; Ghasali, E.; Zabet, M.; Munir, K.S.; Jia, S.; et al. Carbon fiber reinforced metal matrix composites: Fabrication processes and properties. *Compos. Part A Appl. Sci. Manuf.* **2017**, *92*, 70–96. [CrossRef]
2. Akhtar, F.; Askari, S.J.; Shah, K.A.; Du, X.; Guo, S. Microstructure, mechanical properties, electrical conductivity and wear behavior of high volume tic reinforced cu-matrix composites. *Mater. Charact.* **2009**, *60*, 327–336. [CrossRef]
3. Panda, S.; Dash, K.; Ray, B.C. Processing and properties of cu based micro- and nano-composites. *Bull. Mater. Sci.* **2014**, *37*, 227–238. [CrossRef]
4. Rathod, S.; Modi, O.P.; Prasad, B.K.; Chrysanthou, A.; Vallauri, D.; Deshmukh, V.P.; Shah, A.K. Cast in situ cu–tic composites: Synthesis by shs route and characterization. *Mater. Sci. Eng. A* **2009**, *502*, 91–98. [CrossRef]
5. Maity, P.C.; Panigrahi, S.K. Metal and intermetallic matrix in-situ particle composites. *Key Eng. Mater.* **1995**, *104–107*, 313–328. [CrossRef]
6. Casati, R.; Vedani, M. Metal matrix composites reinforced by nano-particles—A review. *Metals* **2014**, *4*, 65. [CrossRef]
7. Islak, S.; Kır, D.; Buytoz, S. Effect of sintering temperature on electrical and microstructure properties of hot pressed cu-tic composites. *Sci. Sinter.* **2014**, *46*, 15–21. [CrossRef]
8. Liang, Y.H.; Wang, H.Y.; Yang, Y.F.; Wang, Y.Y.; Jiang, Q.C. Evolution process of the synthesis of tic in the cu–ti–c system. *J. Alloys Compd.* **2008**, *452*, 298–303. [CrossRef]
9. Dudina, D.V.; Mukherjee, A.K. Reactive spark plasma sintering: Successes and challenges of nanomaterial synthesis. *J. Nanomater.* **2013**, *2013*, 12. [CrossRef]
10. Dudina, D.V.; Mali, V.I.; Anisimov, A.G.; Bulina, N.V.; Korchagin, M.A.; Lomovsky, O.I.; Bataev, I.A.; Bataev, V.A. Ti_3SiC_2-Cu composites by mechanical milling and spark plasma sintering: Possible microstructure formation scenarios. *Met. Mater. Int.* **2013**, *19*, 1235–1241. [CrossRef]
11. Ghasali, E.; Pakseresht, A.H.; Alizadeh, M.; Shirvanimoghaddam, K.; Ebadzadeh, T. Vanadium carbide reinforced aluminum matrix composite prepared by conventional, microwave and spark plasma sintering. *J. Alloys Compd.* **2016**, *688 Pt A*, 527–533. [CrossRef]
12. Ghasali, E.; Shirvanimoghaddam, K.; Pakseresht, A.H.; Alizadeh, M.; Ebadzadeh, T. Evaluation of microstructure and mechanical properties of al-tac composites prepared by spark plasma sintering process. *J. Alloys Compd.* **2017**, *705*, 283–289. [CrossRef]
13. Diouf, S.; Molinari, A. Densification mechanisms in spark plasma sintering: Effect of particle size and pressure. *Powder Technol.* **2012**, *221*, 220–227. [CrossRef]
14. Yang, Y.F.; Mu, D.K. Rapid dehydrogenation of tih2 and its effect on formation mechanism of tic during self-propagation high-temperature synthesis from tih2–c system. *Powder Technol.* **2013**, *249*, 208–211. [CrossRef]
15. Stadelmann, P. Java-Ems: Jems. C2004. Available online: Http://cimewww.Epfl.Ch/people/stadelmann/jemswebsite/jems.Html (accessed on 5 February 2017).
16. Zhuang, J.; Liu, Y.; Cao, Z.; Li, Y. The influence of technological process on dry sliding wear behaviour of titanium carbide reinforcement copper matrix composites. *Mater. Trans.* **2010**, *51*, 2311–2317. [CrossRef]
17. Wang, F.; Li, Y.; Wakoh, K.; Koizumi, Y.; Chiba, A. Cu–Ti–C alloy with high strength and high electrical conductivity prepared by two-step ball-milling processes. *Mater. Des.* **2014**, *61*, 70–74. [CrossRef]